International Journal of Progressive Sciences and Technologies (IJPSAT)
ISSN: 2509-0119.

http://ijpsat.ijsht-journals.org
Vol. 26 No. 1 April 2021, pp. 67-73

Removal of Methyl Violet from Aqueous Solutions using $Sr_2ANbO_{5.5}$ (A= Ca^{+2}, Sr^{+2} & Ba^{+2})

Labib. A. Awin*, Mahmoud. A. El-Rais, Abdunnaser M Etorki, Mokhtar M Abobaker, Mawada. S. Alzorgani, Maryam M. Alnaas, Miloud E Sweesi and Ashraf M. Ward

Chemistry Department, Faculty of Science, Tripoli University, Libya
Chemistry Depertment, , Faculty of Seience, Gharyan,University, Libya
The Faculity of Biotechnology, The University of Aljfara, Libya
Department of Preventive Medicine, Faculty of Veterinary Medicine, University of Tripoli, Libya

Abstract – Three members of the *A*- site doped Nb perovskites with general formula $Sr_2CaNbO_{5.5}$, $Sr_3NbO_{5.5}$ and $BaSr_2NbO_{5.5}$ were synthesised by solid-state methods and their removal efficiency of Methyl violet from aqueous solutions investigated. The X-ray diffraction measurements demonstrated that the three samples have a faced cubic perovskite-type structure in space group $Fm\bar{3}m$. The additions of Ba^{2+} and Ca^{2+} into the *A*-site of $Sr_3NbO_{5.5}$ have influenced the cell volume, crystal size and density. Subsequently, the removal capacity was also impacted. The crystallite size of the three oxides was calculated to be less than 82 nm. The maximum removal capacities of Methyl violet are found to be 46.5, 13.1 and 8.0 mg/g using $BaSr_2NbO_{5.5}$, $Sr_3NbO_{5.5}$ and $CaSr_2NbO_{5.5}$ respectively. The amounts of the adsorbed dye have decreased as the ionic radii of the doped cations decreased. The removals of Methyl violet have positive relationship with pH, temperature and the mass of the oxides.

Keywords – Aqueous, Removal, Methyl violet, *A*-site Doping.

I. INTRODUCTION

The release of wastewater from the textile industry to the environment causes aesthetic problems in the ecosystem. The coloured effluents have a toxic chemical content and influence each temperature, pH and turbidity of water[1]. They usually exhibit high resistance to microbial degradation and remain in the environment for long periods of time. Thus, the treatments of the wastewater have to satisfy: firstly, all coloured effluents are separated from water environment and secondly, that at least a partial or a complete mineralization or decomposition of the coloured wastes. These points can be achieved by physical, biological and chemical processes. The separation methods can be classified based on fluid mechanics to sedimentation, centrifugation, filtration and flotation or on synthetic membrane to nano-filtration and reverse osmosis. Biological methods are used in connection with activated sludge processes and membrane bioreactors. Chemical processes include the advanced oxidation of effluents with ozone or hydrogen peroxide which can be run concomitantly under ultra violet irradiation. Additionally, physical-chemical techniques such as adsorption, chemical precipitation, coagulation, flocculation, and ionic exchange can be used to separate dissolved, emulsified and solid components from the water environment.

Adsorption technique is considered to be one of the most effective treatments of coloured effluents. It is economic and feasible process that generates high quality water[2]. It consists in the transfer of soluble effluents from water to the surface of an adsorbent which is highly porous solid material. Adsorbents can be natural or manufactured organic or inorganic materials. Examples of

Corresponding Author: Labib. A. Awin

natural organic adsorbents are peat and woodchips .Typical Inorganic adsorbents are china clay, bentonite clays, silica gel, zeolites and metal oxides[3]. Many efforts have been applied to synthesize and develop new materials as adsorbents. One of these is the use of mixed metal perovskite type oxides. Perovskites with general formula ABO_3 are fascinating class of multifunctional materials. They exhibit a wide variety of physical properties such as optical, magnetic, electric and catalytic. Such properties can be controlled by variations in *A* and *B* cations[4].

This paper presents the removal of Methyl Violet from aqueous solutions using $Sr_2ANbO_{5.5}$ (*A*= Ca^{2+}, Sr^{2+} and Ba^{2+}). Methyl violet 10B (MV) is known in medicine as Gentian violet and is the active ingredient in a Gram stain, used to classify bacteria[5]. It is used as a pH indicator, with a range between 0 and 1.6. Compounds related to methyl violet are potential carcinogens. Methyl violet 10B inhibits the growth of many Gram positive bacteria, except streptococci. It is soluble in water, ethanol, diethylene glycol and dipropylene glycol. Methyl violet is a mutagen and mitotic poison, therefore concerns exist regarding the ecological impact of the release of methyl violet into the environment[5]. Methyl violet has been used in vast quantities for textile and paper dyeing, and 15% of such dyes produced worldwide are released to environment in wastewater.

In the $Sr_2ANbO_{5.5}$ perovskite oxides, the high polarizing cations Ca^{2+}, Sr^{2+} and Ba^{2+} fairly occupy the octahedral site obtaining a rocked salt ordering in the structure[6]. The ordered-cation distribution is attributed to the differences in both the ion size and the bonding character of the *B*-site cations[7, 8]. The partial substitution of Sr^{2+} was expected to influence the oxide structure leading to changes in the physical properties. These physical properties can be influenced by the differences in the ionic radii and the electron configurations of the doped cations. In such semiconductor nanoparticle oxides, particle size, shape and surface states are the predominant factors, which influence its properties such as adsorption[9].

II. Experimental

Sample preparation

The preparation of samples involved Nb_2O_5 (Merck, 99.99%), $SrCO_3$ and/or $CaCO_3$, $BaCO_3$ (BDH, 99.98-99.99%). The appropriate stoichiometric amounts were mixed, using a mortar and pestle, and then heated in several steps with intermittent regrinding. Samples were initially heated at 850°C for 12 h followed by reheating at 1100°C for 48 h.

Instrumentations

The crystallography of the samples was examined by a PANalytical X'Pert X-ray powder diffraction using Cu Kα radiation (1.5400 Å) and a PIXcel solid-state detector. The operating voltage was 40kV and the current was 30 mA. The samples were measured in lat plate mode at room temperature with a scan range of 10°<20°<80° and a scan length of 10 mins were used. The structures were refined using the program RIETICA[10].

The absorbance of solutions was determined using ultraviolet visible spectrophotometer (UV/Vis, model Spect-21D) and (190-900 Perkin- Elmer) at maximum wavelength of absorbance (590 nλ). The concentrations of solutions were estimated from the concentration dependence of absorbance fit. The pH measurements were carried out on a WTW720 pH meter model CT16 2AA (LTD Dover Kent, UK) and equipped with a combined glass electrode.

Batch mode

Batch mode removal studies were carried out by varying several parameters such as contact time, pH, temperature and mass of prepared oxide (adsorbent). Essentially, a 50 ml of dye solution with concentration of 10 ppm was taken in a 250 ml conical flask in which the initial pH was adjusted using HCl/NaOH. Optimized amount of adsorbent was added to the solution and stirred using magnetic stirrer for specific time. The oxide samples were separated from solutions using centrifuge 3500 CPM for 5 minutes.

III. Result and Discussions:

3.1. Characterization of oxides

X-ray diffraction patterns (Figure 1) demonstrated the three oxides to have a faced cubic structure with space group ($Fm\bar{3}m$). The substitution of Sr^{2+} by either Ca or Ba has resulted in significant changes in cell volumes, density, crystallite and surface area. For instance, doping with Ba^{2+} significantly increases the cell volume from 577.230 to 604.520 $Å^3$ where doping with Ca^{+2} has decreased the cell volume to 559.490 $Å^3$. This is likely driven by the large ionic size of the Ba^{2+} cation (12 coordinate ionic radius,

1.61 Å) and the small ionic size of the Ca^{2+} cation (12 coordinate ionic radius, 1.34 Å). The ionic size of the Sr^{2+} cation (12 coordinate ionic radius, 1.44 Å) is smaller than the Ba^{2+} cation but is larger than the Ca^{2+} cation. Table 1 displays the average Crystallite size, specific surface area, lattice strain, lattice parameter and Cell volume as estimated from X-ray diffraction data for the oxides. The increase in the cell volume, specific surface areas and densities of the oxides is consistent with the increase in the ionic radii of the doped divalent cations Ca, Sr and Ba. The crystallite size can be calculated using sheerer formula[11] (Equation. 1) where the specific surface area can be calculated using Sauter formula[12] (Equation.2) in which ρ is the density of the synthesised material.

$$D_p = (0.94\lambda)/(\beta_{1/2} \times \cos\Theta). \quad (1)$$

$$S = 6000/ (D_p \times \rho). \quad (2)$$

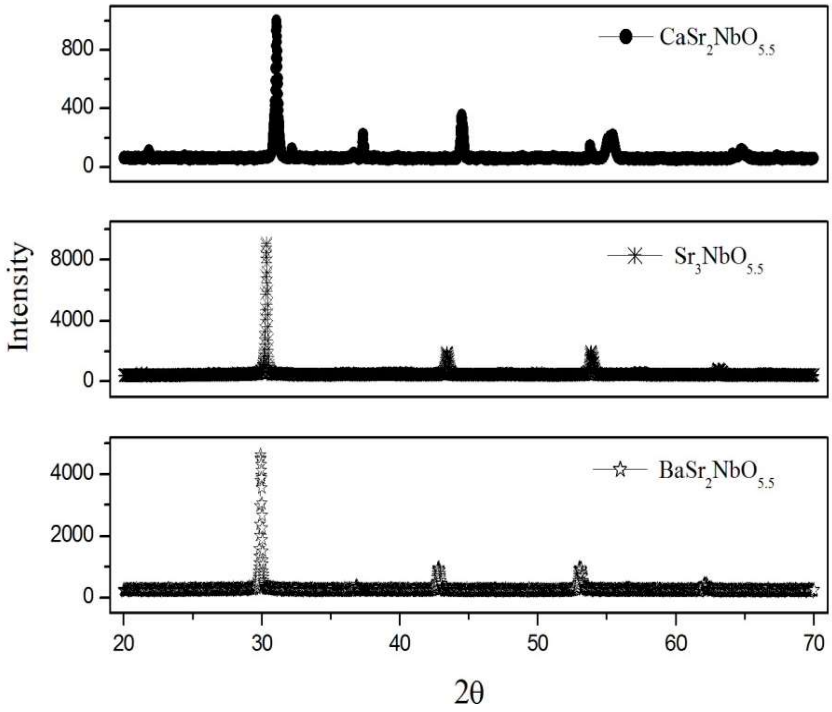

Figure-1 the XRD patterns of Sr2CaNbO5.5, Sr3NbO5.5 and BaSr2NbO5.5.

Table-1; Average Crystallite size Dp, Specfic surface area S, lattice strain φ, Lattice parameter a and Cell volume V. estimated from X-ray diffraction data.

Formula	D_p (ηm)	ρ(g/cm³)	S (m²/g)	φ	a (Å)	V (Å³)
$Sr_2CaNbO_{5.5}$	50.45	4.70	13.64	0.0015	8.2401(2)	559.490(1)
$Sr_3NbO_{5.5}$	81.91	5.104	14.35	0.0028	8.3263(3)	577.230(1)
$BaSr_2NbO_{5.5}$	50.45	5.419	22.03	0.0020	8.4554(2)	604.520(1)

$BaSr_2NbO_{5.5}$ and $Sr_2CaNbO_{5.5}$ displayed a similar crystallite size, possibly as a consequence of cation order effects. The materials can be formulated as (BaSr)$SrNbO_{5.5}$ and (SrSr)$CaNbO_{5.5}$ in order to emphasize the ordering at the *B* site between the Sr and/or Ca with Nb cations. In the double perovskite structure, it is anticipated that the two smallest cations will order in the octahedral sites, this ordering being a consequence of the differences in the size and/or charge between the two cations. The largest cation will then occupy the 12-coordinate (cuboctahedral) site. The corresponding ionic radii of Ba^{2+} (12 coordinate ionic radius, 1.61 Å and 6 coordinate ionic radius. 1.35 Å[13]); Sr^{2+} (1.44 and 1.18 Å[13]); Ca^{2+} (1.34 and 1.00 Å[13]); and Nb^{5+} (6 coordinate ionic radius. 0.64

Å[13]) cations suggest that the Nb^{5+} and one Sr^{2+} or Ca^{2+} cation will occupy the 6-coordinate sites whereas Sr^{2+} or a mixture of Sr^{2+} and Ba^{2+} will occupy the cuboctahedral sites[8].

3.2. Batch mode

3.2.1 Effect of Time.

The removal percentage of dyes over the adsorbents can be calculated as: $R\% = [(C_i-C_t)/C_i] \times 100$, where R% is the removal percentage, C_i = 10 ppm is initial concentration of dye solution, C_t is the concentration of dye at contact time estimated from the concentration dependence of absorbance fit. Figure 2 shows the time dependence of MV removal at room temperature. There is no finite time was observed for the dye removal up to 150 min. The removals of the dye increase as the contact time increases. The removal of MV on the surface of $Sr_2CaNbO_{5.5}$, $Sr_3NbO_{5.5}$ and $BaSr_2NbO_{5.5}$ were found to be 79.80, 66.15 and 73.24 % respectively. The removals of MV using the doped oxides $Sr_2CaNbO_{5.5}$ and $BaSr_2NbO_{5.5}$ were larger than that of the undoped oxide $Sr_3NbO_{5.5}$. This result reflects the importance of the element composition and the element substitution in the enhancement of the adsorption properties of such oxides. Generally, the increase in the removal is consisted with the decrease in the crystallite size of the oxides. The inserted equations in Figure 2 describe the removal percentage (R%) as function of time (t) for each oxide. The initial removal rate (dR/dt) could be derived from the equations when t=0. The initial removal rates for MV dye were found to be 35.4, 27.7 and 27.2 using $Sr_2CaNbO_{5.5}$, $Sr_3NbO_{5.5}$, and $BaSr_2NbO_{5.5}$ respectively. The wavelength dependence of absorbance for MV solution (Figure 2) illustrates the absorbance of MV solutions decreased as result of using the oxides as adsorbents.

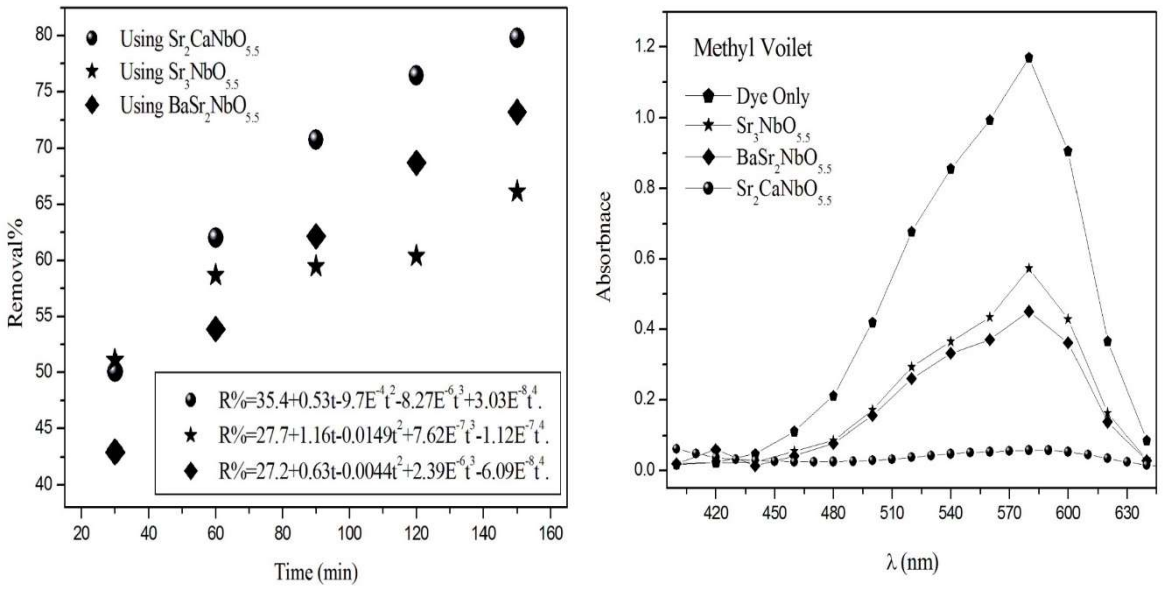

Figure 2. the time dependence of MV removal and The wavelength dependence of absorbance for MV solution at room temperature. The volume, concentration and pH of the dyes solution are 50ml, 10ppm and 5.1 respectively.

3.2.2: Effect of adsorbent mass

The amount of the dye adsorbed by one gram of the oxides (Q) was calculated as following: $Q\ (mg/g) = [(C_i-C_t)\times V]/W$, where t= 150 min is the contact time, V= 50 ml is the volume of MV solution and W is the mass of oxides. As shown in Figure 3, Q decreases as the mass of adsorbents increased. The maximum capacity of adsorbent Q_{max} can be estimated from the intercept of the liner fit of $1/Q_t$ at Y axis. $Sr_2CaNbO_{5.5}$ (50.45 nm, 13.64 m^2/g) displayed the highest value of Q_{max} (47.39(2) mg/g) whereas $Sr_3NbO_{5.5}$ (81.91 nm, 14.35 m^2/g) exhibited the lowest value of Q_{max} (8.03(5) mg/g). Q_{max} for $BaSr_2NbO_{5.5}$ (50.45 nm, 22.03 m^2/g) is 13.09(2) mg/g. This result reflects an enhancement in the adsorption properties has occured as result of the substitution of Ca^{2+} and Ba^{2+} into $Sr_3NbO_{5.5}$.

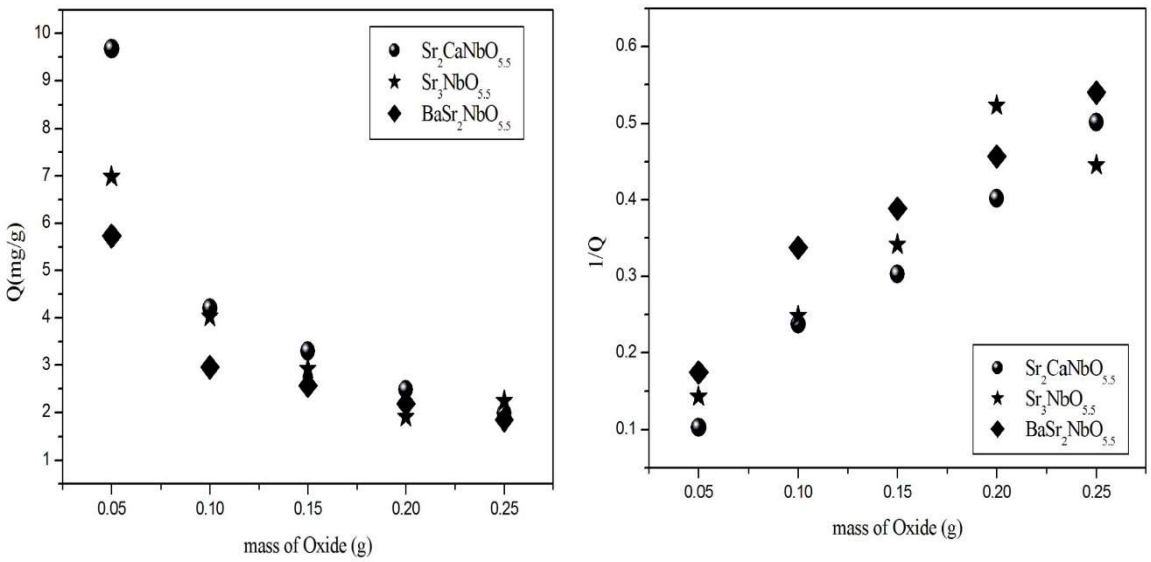

Figure 3. The effect of adsorbent mass on the removal. The time, volume, concentration and pH of dye solutions are 150min, 50ml, 10ppm and 5.1 respectively.

3.2.4: Effect of temperature

Temperature has an important impact on the adsorption process. An increase in temperature helps the reaction to compete more efficiently with e^{-}/H^{+} recombination. The removal of two dyes was investigated at 25, 40, 60 and 100°C. The obtained results are illustrated below in Figure 4. The removal of MV dye increased as temperature increased. For instance, the removal of MV increased from ~84% at 25°C to ~99% at 100°C when $Sr_2CaNbO_{5.5}$ was used. This result is agreed with normal expectations, and is a consequence of the increase of adsorption strength and the concentration of active intermediates with temperature. The energy of activation (E_a), was calculated from the Arrhenius plot of ln R vs 1000/*T*. Arrhenius plot shows that the activation energies of the removal are positive and equal to 1.77, 4.79 and 4.32 kJ/mole for $Sr_2CaNbO_{5.5}$, $Sr_3NbO_{5.5}$ and $BaSr_2NbO_{5.5}$ respectively. This suggests that doping with Ca and Ba has resulted in lower activation energy for the process. The activation energy of the removal using $Sr_2CaNbO_{5.5}$ is lower than that observed for $BaSr_2NbO_{5.5}$.

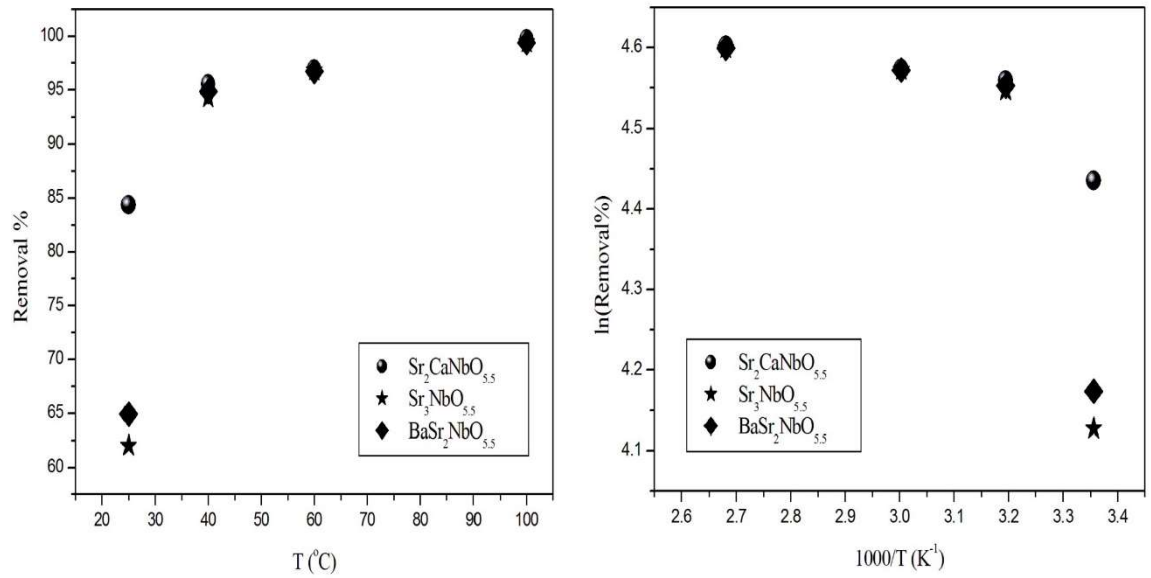

Figure 4. the effect of temperature on the MV removal. The time, volume, pH and concentration of dyes solutions are 150min, 50ml, 5.1 and 10ppm respectively

3.2.4: Effect of pH

The pH of solutions is a key parameter in dye adsorption. The magnitude of electrostatic charges which are impacted by the ionised dye molecules is controlled by the solution pH. As a result the rate of adsorption will vary with the pH of the medium used. In general, at low solution pH, the percentage of dye removal will decrease for cationic dye adsorption, while for anionic dyes the percentage of removal will increase. This is due to the increase in the positive charge on the solution interface and the adsorbent surface. In contrast, high solution pH is preferable for cationic dye adsorption but shows a lower efficiency for anionic dye adsorption. The positive charge at the solution interface will decrease while the adsorbent surface appears negatively charged.

To study the effect of pH, experiments were carried out at various pH values, ranging from 2 to 10 for constant dye concentration (10 ppm) and adsorbent mass (0.1g). Figure 5 presents the removal of dyes as a function of pH. It was observed that the removal of MV using $Sr_3NbO_{5.5}$ has gradually increased from ~50% to ~75% as pH increased from 2 to 10. In contrast, the removal of MV using $Sr_2CaNbO_{5.5}$ gradually decreases as pH increased from 4 to 10. The removal of MV using $BaSr_2NbO_{5.5}$ steadly decreases as pH increased from 2 to 10. The highest removal of MV was recorded at pH= 2 (~90 %) using $BaSr_2NbO_{5.5}$ whereas the lowest removal was recorded at pH=2 (~33%) when $Sr_2CaNbO_{5.5}$ was used. The removal efficiency of the adsorbents is clearly increases as the acidity decreased.

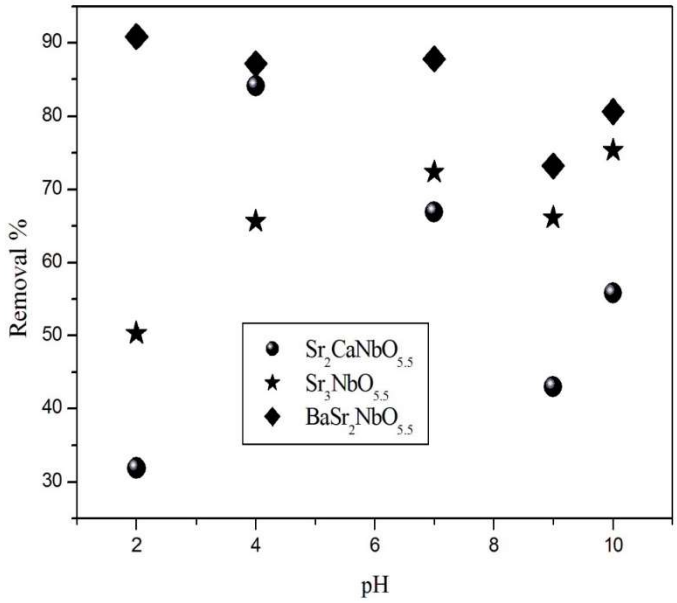

Figure 5. the effect of pH on the removal of MV. The time, volume and concentration of dyes solution are 150min, 50ml and 10ppm respectively.

IV. Conclusion

The removal of Methyl Violet from aqueous solution using the *A*- site doped perovskites $Sr_2ANbO_{5.5}$ (*A*= Ca, Sr or Ba) has been reported. The nano particle materials were made by solid state method and characterized by XRD. The results showed the substitutions of Ca^{2+} and Ba^{2+} have impacted both the structural and adsorption properties of the oxides. It was found that the removal of Methyl Violet increases as result of the divalent cation doping. The removal of MV increases as the physical parameters: time, temperature and adsorbent mass increased. The maximum capacities of adsorbent are 47.39, 13.09 and 8.03 mg/g for $Sr_2CaNbO_{5.5}$, $BaSr_2NbO_{5.5}$ and $Sr_3NbO_{5.5}$ respectively. The highest removal efficiency was recorded for MV dye using $BaSr_2NbO_{5.5}$ at pH=2 where the lowest removal was observed at same pH for $Sr_2CaNbO_{5.5}$.

References

[1] Agarwal S. K., Water Pollution, A.P.H. Publishing Corporation, 2005.

[2] Cheremisinoff N. P., Handbook of Water and Wastewater Treatment Technologies, Butterworth-Heinemann, 2002.

[3] Pawlowski L., Physicochemical Methods for Water and Wastewater Treatment, Elsevier Science, 1982.

[4] Tejuca L. G. and Fierro, J. L. G., Properties and Applications of Perovskite-Type Oxides, Taylor & Francis, 1992.

[5] Books H., Articles on Triarylmethane Dyes, Including: Phenolphthalein, Methyl Violet, Bromothymol Blue, Coomassie Brilliant Blue, Bromophenol Blue, Malachite Gr, Hephaestus Books, 2011.

[6] Lecomte J., Loup, J. P., Hervieu, M. and Raveau, B., "Non-stoichiometry and electrical conductivity of strontium niobates with perovskite structure", Physica Status Solidi, 2, 65, 743-752, 1981.

[7] Animitsa I., Neiman, A., Sharafutdinov, A. and Nochrin, S., "Strontium tantalates with perovskite-related structure", Solid State Ionics, 0, 136–137, 265-271, 2000.

[8] King G. and Woodward, P. M., "Cation ordering in perovskites", Journal of Materials Chemistry, 28, 20, 5785-5796, 2010.

[9] Fergus J. W., "Perovskite oxides for semiconductor-based gas sensors", Sensors and Actuators B: Chemical, 2, 123, 1169-1179, 2007.

[10] Hunter B. A. and Howard, C. J., "RIETICA. A Computer Program for Rietveld Analysis of X-Ray and Neutron Powder Diffraction Patterns", Rietica, 1998.

[11] Langford J. I. and Wilson, A. J. C., "Scherrer after sixty years: A survey and some new results in the determination of crystallite size", Journal of Applied Crystallography, 2, 11, 102-113, 1978.

[12] Nogi K., Hosokawa, M., Naito, M. and Yokoyama, T., Nanoparticle Technology Handbook, Elsevier, 2012.

[13] Shannon R. D., "Revised Effective Ionic-Radii and Systematic Studies of Interatomic Distances in Halides and Chalcogenides", Acta Crystallographica Section A, Sep1, 32, 751-767, 1976.